

Physical and Chemical Properties of Galactic Global Clusters with Various Origins Identified from the Gaia DR2 Data

V. A. Marsakov^{a,*}, V. V. Koval^{a,**}, and M. L. Gozha^{a,***}

^a*Southern Federal University, Rostov-on-Don, 344006 Russia*

**e-mail: marsakov@sfedu.ru*

***e-mail: vvkoyal@sfedu.ru*

****e-mail: gozha_marina@mail.ru*

Received April 20, 2020; revised June 8, 2020; accepted June 30, 2020

Abstract—The differences in the relationships between the physical parameters and the chemical-element abundances in accreted globular star clusters and those formed inside the Galaxy have been investigated. The information on the supposed formation sites of the clusters based on the Gaia DR2 data is borrowed from the literature. Those sources estimate the probability of belonging to the Galactic bulge and disk, as well as to six known events of the merger of dwarf satellite galaxies with the Milky Way, for 151 globular clusters. Orbital elements, initial masses, population types, and ages are taken from the literature; the data on the chemical composition for 69 globular clusters of the Galaxy are taken from the authors' compiled catalog. It is shown that all metal-poor ($[\text{Fe}/\text{H}] < -1.0$) genetically related globular clusters have high relative abundances of α -elements. According to modern views, since type II supernovae release more α -elements into the interstellar medium with increasing mass, it has been suggested that masses of type II supernovae in the Galaxy were greater than in the accreted galaxies. It is proved that the clusters of the low-energy group, which were considered accreted, are genetically related to a single protogalactic cloud, same as the unstratified clusters UKS 1 and Liller 1, which most likely belong to the bulge. It is shown that not only the lower but also the upper limits of the clusters' masses decrease with an increase in the average radius of their orbits. The latter fact is explained by a decrease in the masses of emerging clusters with a decrease in the masses of their host galaxies. It is demonstrated that an extremely multicomponent stellar population is observed only in accreted globular clusters with an initial mass $>10^6 M_{\odot}$. It has been suggested that these clusters retained all the matter ejected by their evolved stars, from which new generations of stars formed due to long evolution far from our Galaxy.

DOI: 10.1134/S1063772920110062

1. INTRODUCTION

According to the modern standard cosmological model Λ CDM (Lambda-Cold Dark Matter), the masses of galaxies grow due to mergers. The galactic halo forms as a result of several large mergers, accompanied by numerous small ones. When satellites merge with a galaxy like the Milky Way, they lose their stars due to tidal forces. These stars follow approximately the mean orbit of their progenitor, and this leads to stream formation.

In recent years, observational astronomy has provided us with some compelling evidence that not all stars that currently belong to our Galaxy formed from the same protogalactic cloud. Some stellar objects were captured from the nearest satellite galaxies. The accretion epoch of extragalactic objects began at the earliest stages of the Galaxy formation and continues to this day [1]. The presumably accreted objects can be identified more or less reliably only after measuring their spatial velocities and recovering their galactic orbits. A necessary condition for verifying their extra-

galactic origin is to determine their abundance of chemical elements produced in various processes of nuclear fusion. The fact is that isolated star–gas systems may have different chemical evolution histories.

To identify field stars and globular clusters with a common origin, their dynamic properties in the integral space of motion and their chemical composition are analyzed based on the Gaia data. Mackereth et al. [2] analyzed relative abundances of α -elements and velocities of tens of thousands of stars within 15 kpc from the Sun in a sample compiled by cross-identification between the SDSS-APOGEE DR14 and Gaia DR2 catalogs. The authors found that in metal-rich ($[\text{Fe}/\text{H}] > -1.0$) stars with high orbital eccentricities, the $[\alpha/\text{Fe}]$ ratios are lower than those of the majority of the nearest field stars. As a result, it was concluded that our Galaxy at the early stages of its evolution captured a massive ($\sim 10^9 M_{\odot}$) satellite galaxy; as a result, part of the field stars born in the satellite entered our Galaxy, and part of the stars of the already formed thin

disk “heated up”, forming a subsystem of the thick disk. The same conclusion was reached by Helmi et al. [3], who used the APOGEE and Gaia DR2 surveys, as well as numerical simulations, to show that fragments of a dwarf galaxy more massive than the Small Magellanic Cloud, which the authors named Gaia–Enceladus, predominate in the inner halo. They found that among the stellar objects they studied, hundreds of RR Lyraes and more than a dozen globular clusters formed in that galaxy. Moreover, the merger of the Milky Way with Gaia–Enceladus, in their opinion, led to the dynamic “heating” of the predecessor of the thick galactic disk and, therefore, contributed to the formation of this Galaxy subsystem approximately 10 Gyr ago. However, the Gaia–Enceladus remnants are not the only substructure present in the neighborhood of the Sun. In particular, the solar region is traversed by the Helmi streams 99 discovered more than 20 years ago. Moreover, quite recently, the Gaia DR2 and DECaPS data revealed the evidence of not one but two captures of massive galaxies approximately 9–11 Gyr ago.

Massari et al. [4] studied the integrals of motion (see below for more details) and ages of Galactic globular clusters based on the Gaia DR2 data and the derived parameters of galactic orbits; these studies show that approximately 40% of globular clusters probably formed “in situ”, i.e., are genetically related to a single protogalactic cloud. More than a third (35%) of the clusters are apparently associated with known merger events, in particular with the Gaia–Enceladus galaxy (19%), the Sagittarius dwarf galaxy (5%), the progenitor of the Helmi 99 streams (6%), and the Sequoia galaxy (5%), although there is still some uncertainty due to the degree of overlapping in their dynamic characteristics. Sixteen percent of the remaining clusters are associated with low-energy and high-energy groups, while the rest lie in greatly elongated orbits very high above the galactic plane, so they are most likely of heterogeneous origin.

In [5–7], we calculated the probabilities of the clusters belonging to the subsystems of the thick disk and halo using the method described by Bensby et al. [8] with the aid of ground-based measurements of their residual velocities. Only the clusters that belonged to the thick disk were considered to be genetically related to a single protogalactic cloud; as for the halo, we kept only the clusters in direct orbits within 15 kpc from the galactic center. The studies showed, in particular, that the entire set of accreted clusters in the $[\text{Fe}/\text{H}]$ – $[\alpha/\text{Fe}]$ diagram in the range of $[\text{Fe}/\text{H}] < -1.0$ occupies nearly the same band as fast ($V_{\odot} > 240$ km/s), i.e., accreted field stars. At the same time, almost all genetically related clusters, as well as accreted clusters that belonged in the past to two disrupted massive dwarf galaxies Sgr and CMa, are concentrated towards the upper part of this band, together with genetically related field stars ($V_{\text{res}} < 240$ km/s).

The stars of the current dwarf satellite galaxies of our Galaxy with the same low metallicity have significantly smaller $[\alpha/\text{Fe}]$ values. As a result, it was concluded that all stellar objects of the accreted halo are remnants of galaxies with a higher mass than the current environment of the Galaxy.

Since we previously identified clusters as presumably accreted and genetically related based on error-burdened ground-based measurements of their distances and velocities, in this study we will use the stratification performed by Massari et al. [4] based on more accurate satellite data. These data made it possible to determine the velocities and thus calculate the orbits of almost all known globular clusters that currently belong to our Galaxy, thereby significantly increasing the number of globular clusters used for the analysis. In this study, we are interested in the difference between the physical and chemical properties of sets of genetically related clusters and accreted clusters, as well as possible differences in properties between various presumably accreted cluster groups.

2. INITIAL DATA

2.1. Chemical Element Abundances

To analyze the behavior of some chemical elements in globular clusters, we took spectroscopic determinations of iron abundances and the relative abundances of some chemical elements from our compiled catalog [5], which includes an earlier catalog by Harris [9]. Our catalog contains the averaged abundances of 28 chemical elements in the stars of 69 globular clusters from 101 articles published from 1986 to 2018. It is known that all the clusters underwent self-enrichment, which changed their averaged stellar abundances of some chemical elements (see e.g., [10] and references therein). The distorted abundances are mainly of those chemical elements that are involved in the reactions of proton captures occurring in the hydrostatic helium burning in the center or in the layer sources of the asymptotic-branch giants. When such a star sheds its shell at later evolution stages, these elements enter the interstellar medium of the cluster. As a result, new generations of stars have an altered chemical composition. The average abundances of other chemical elements in the cluster stars remain almost unchanged (see, e.g., [11] and references therein). This allows us to use the averaged stellar abundances of the undistorted chemical elements in the clusters to study the nature of each globular cluster.

In this paper, we consider the behavior of almost undistorted relative abundances of four α -elements (magnesium, silicon, calcium, and titanium) as the most informative in terms of diagnosing the evolution of the early Galaxy, as well as one rapid neutron capture element, europium. In [5], we gave a detailed description of the procedure for averaging the relative abundances of each element and their errors. At the

same time, we demonstrated that the external convergence of the abundances determined by different authors lied in the range $\langle \sigma_{[el/Fe]} \rangle = (0.06-0.11)$ and deemed possible to use our compiled abundances of chemical elements for the statistical analysis of the initial chemical composition of clusters belonging to different Galactic subsystems. Since spectroscopic data are known for less than half of globular clusters, we used metallicities from the computer version of Harris' compiled catalog [9], in which they are given for almost all clusters, to analyze the relationships between physical parameters and heavy-element abundances.

For comparison, we used field stars from the catalog [12], which lists the metallicities and relative abundances of all α -elements, as well as europium, for 785 stars of the Galaxy in the entire metallicity range of our interest. The silicon abundances are not given; for this reason, they are taken from the catalog [13], which contains 714 F–G field dwarfs. Unfortunately, the latter catalog contains stars belonging mainly to the disk populations of the Galaxy, so metal-poor stars in it are few.

2.2. Principles of Determining Birthplaces of Globular Clusters

Massari et al. [4] considered the positions of all clusters in the space of calculated integrals of motion: total orbital energies (E), angular momentum components (L_Z), angular momentum components (L_{\perp}) perpendicular to L_Z , and other elements of the cluster galactic orbits. At the same time, each cluster was analyzed for relations to a single protogalactic cloud and to the progenitors of the known merger events experienced by the Galaxy. The clusters that were born, in the authors' opinion, within the Galaxy (in situ) were restricted by additional parameters. The bulge clusters should satisfy the condition $R_{\max} < 3.5$ kpc (36 clusters of this subsystem were identified as a result), while the clusters belonging to the disk subsystem were restricted by the low elevation of the orbital points above the galactic plane ($Z_{\max} < 5$ kpc) and small eccentricities of galactic orbits. Among the 26 identified disk clusters, several were in retrograde orbits. The authors found that all "pure" in situ clusters show a greater age given the same metallicity. For this reason, they excluded two relatively young clusters (NGC 6235 and NGC 6254) from this group. Thus, in addition to the integrals of motion, the ages of globular clusters were also considered during the stratification (see below for more details). Note that due to the large scatter of the dynamic characteristics of the Gaia–Enceladus group and their overlapping with the parameters of other groups, the authors of the cited work had to keep double affiliation for some clusters. As a result, in our diagrams, such clusters are indicated

by two superimposed symbols. The stratification for all the clusters is given in [4, Table 1].

Recall that in [5–7], we identified clusters as genetically related (i.e., born from the same protogalactic cloud) if they were in direct orbits and stayed within 15 kpc from the galactic center. In addition, these clusters should demonstrate the same residual velocities as the field stars of the Galaxy's disk subsystems (i.e., close to circular) and not be considered the remnants of known satellite galaxies disrupted at that time. Although we considered all counter-orbiting clusters to be accreted, nevertheless, the majority of clusters identified as genetically related using such different approaches to kinematic data coincided (compare Table 1 in [4] and [6]). Note that, unlike Massari et al. [4], we added the bulge clusters to the thick disk, while those authors had all the stellar objects of the proper halo subsystem in the disk subsystem.

2.3. Cluster Ages

The ages for 68 globular clusters are also taken from [4]. The authors of that study scaled all the relative ages determined by different authors from modern photometric data to a uniform scale of absolute ages by VandenBerg et al. [14], which is based on the spectroscopic scale for determining the abundances of chemical elements by Carretta et al. [15].

2.4. Cluster Type by Multicomponent Population

It has long been known that stellar populations in all globular clusters are not chemically homogeneous and contain at least two generations of stars (1G and 2G). The second population formed from the ejections of evolved stars from the first generation, and is characterized by increased abundances of proton capture elements. However, there are also clusters that show two or more parallel sequences of 1G and 2G stars. Using the Hubble Space Telescope UV Legacy Survey of Galactic Globular Clusters, Marino et al. (see [16] and references therein) divided the globular clusters into two groups based on their multicomponent stellar population. This division was made according to spectroscopic abundances of the chemical elements in the cluster stars. For the study, we took all the seven clusters listed in [16] with an extremely multicomponent Type II population: NGC 362, NGC 1851, NGC 5286, NGC 6656, NGC 6715 (M 54), NGC 7089 (M 2), and NGC 5139 (ω Cen).

2.5. Cluster Masses

Until recently, the masses of clusters were determined from their total luminosity. Now that Gaia DR2 data have become available and it is possible to determine not only total velocities, but also velocities of individual stars even for the most distant clusters, the masses are calculated from the velocity dispersions

of these stars. Based on these data, Baumgardt et al. [17] figured the following: determined the dispersions within 154 globular clusters; calculated their current masses and galactic orbits; and recovered their initial masses (M_{ini}) considering the loss of stars by each cluster over its lifetime as a result of interaction with inhomogeneities of the galactic potential and dissipation of stars. From that study, we took the current and initial masses of the clusters, as well as the average radii of their orbits.

2.6. Morphological Index

The morphological index, or the horizontal branch color $\text{HBR} = (B - R)/(B + V + R)$, where B , V , R are, respectively, the number of stars at the blue end of the horizontal branch, in the instability band, and at the red end, is taken from our catalog [5].

3. RELATIONS BETWEEN THE PHYSICAL CHARACTERISTICS OF CLUSTERS

Figure 1a shows the relationship between the age and metallicity of clusters (the latter is taken from the catalog [9], since it is available for all clusters). The symbols mark the clusters belonging to all nine groups distinguished in [4]. Clusters of different groups are indicated with different symbols; large spheres denote the clusters formed within the Galaxy (in situ). The diagram clearly shows two parallel dependences differing in age. Note that the authors of [14], who were the first to discover this structure in the diagram, did not find an unambiguous explanation of the nature of these two sequences, but linked their occurrence to the difference in the loss of gas ejected by the asymptotic-branch giants of the clusters. It is clearly seen that with a fixed metallicity, the genetically related globular clusters of the bulge and disk are older than the clusters, which, based on their spatial-kinematic properties, the authors of [4] assumed to be accreted from several disrupted satellite galaxies. The sequence intersection of clusters with different origin in the diagram is observed only for the oldest metal-poor clusters. The authors of [4] considered the difference in ages to be the main signs (along with the kinematics) of their extragalactic origin. Clusters with an extremely multicomponent population are highlighted in the same diagram. It can be seen that all of them are among accreted clusters.

In Fig. 1b, the current mass of the clusters (black dots) and the calculated initial masses (large symbols) dependences versus the average radii of their orbits are plotted based on the data of [17]. There is a sharp difference between the initial and current masses of the clusters whose average radii of the orbits lie within the solar circle. The authors of the cited work explained the absence of clusters with initially low mass at small galactocentric distances by their complete disruption to date. At the same time, with an increase in the aver-

age radius of their orbits, the lower limit of the initial mass monotonically increases due to the reduced destructive effect from the bulge and the disk of the Galaxy. Note that the excess of low-mass globular clusters at large galactocentric distances detected from current masses has been known for a long time [18].

Another noteworthy feature in the figure is a decrease in the upper boundary of the initial mass of clusters with increasing orbital radius, which becomes sharper outside the solar orbit radius (see the vertical dashed line). The exception is three initially massive clusters from the disrupted Sagittarius galaxy; one of them (M 54) was presumably the nucleus of this galaxy. Central clusters of galaxies have a special formation history; they lose almost no stars due to dissipation, and can also increase their mass due to the field stars of the parent galaxy falling on them until the disruption of the latter. All clusters with distant orbits ($R_{\text{sr}} > R_{\odot}$) and initial masses below the average (see the horizontal dashed line) were accreted. It turns out that massive globular clusters are less likely to form in dwarf galaxies. Although the Gaia–Enceladus galaxy was still very massive, judging by the number of massive clusters in it, it was nevertheless inferior to our Galaxy. This assumption is consistent with the authors' conclusion of [3], who argued that our Galaxy captured a galaxy with a stellar mass $\sim 6 \times 10^8 M_{\odot}$ approximately 10 Gyr ago. A special situation is with the progenitor of the low-energy group, in which the masses of globular clusters are even greater than those of the disk group clusters, but the orbital radii are smaller. The authors of [4] considered this group to be the remnants of some disrupted dwarf galaxy, since they all lie on the metallicity–age diagram in the same band as all accreted younger clusters (see Fig. 1a). However, as can be seen from the same figure, the lowest-metallicity clusters, which make up more than half of this group (7 out of 13), lie with the oldest disk clusters. And only more metallic clusters ($[\text{Fe}/\text{H}] \geq -1.6$) turn out to be younger than the bulge and disk clusters. For this reason, we believe the origin of this group of clusters is doubtful (see below). Figure 1b also makes it possible to suggest the origin of three globular clusters unstratified in [4]. In particular, the small average orbital radii and high masses of the UKS 1 and Liller 1 clusters indicate that they most likely belong to the bulge subsystem, while the very distant low-mass cluster (AM 4) is almost certainly accreted.

The large triangles in Fig. 1b mark the Type II clusters, which, according to the authors of [16], have extremely multicomponent populations. These clusters, as we can see, are all accreted; initially they had masses of more than a million solar masses, and all of them, except for two former nuclei of satellite galaxies (ω Cen and M 54), lie in orbits with radii close to the solar radius. All these clusters are captured from disrupted dwarf satellite galaxies; i.e., in the initial period

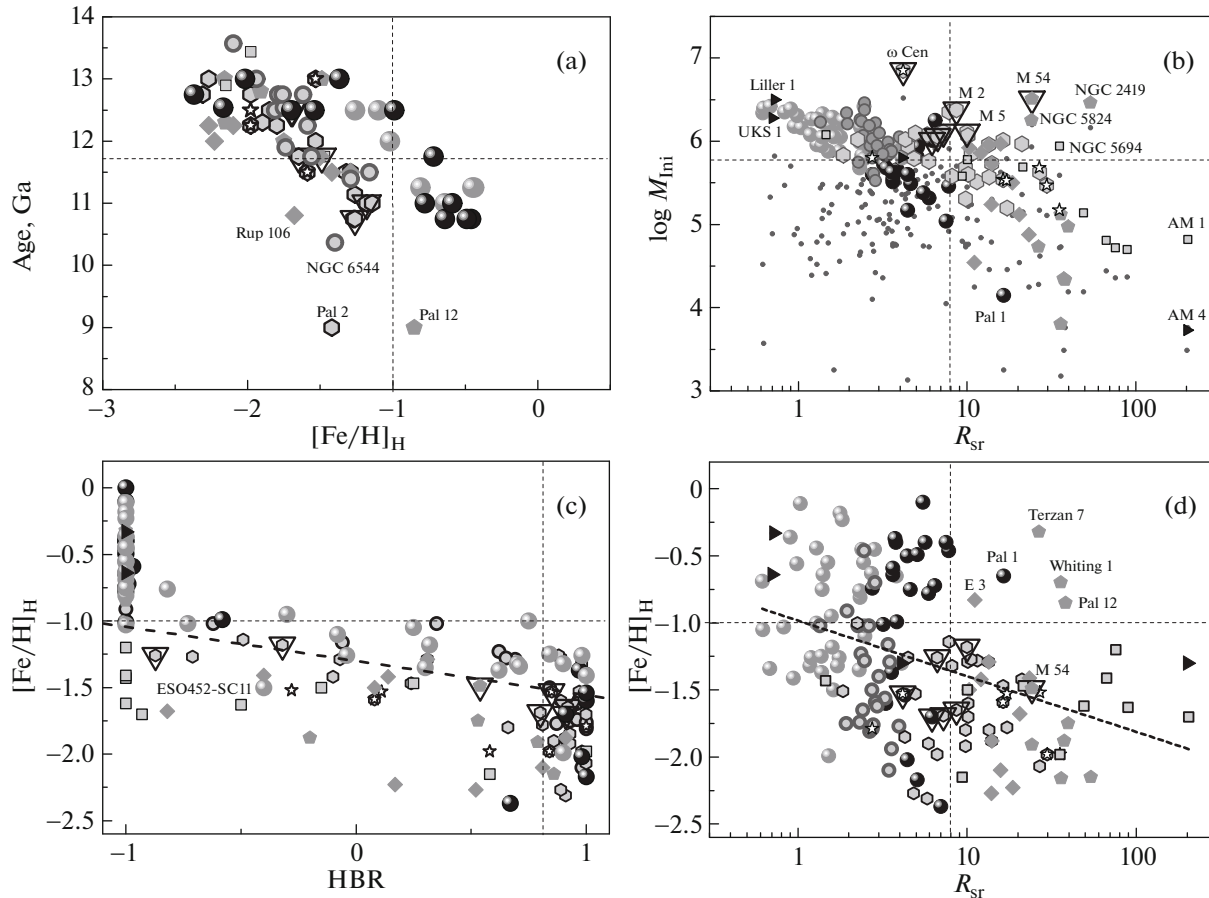


Fig. 1. Relationship between (a) metallicity and age; (b) average orbital radius and initial mass; (c) morphological index of the horizontal branch and metallicity; and (d) average orbital radius and metallicity for globular clusters of various origins. Genetically related globular clusters are indicated by large spheres: the light spheres are bulge clusters, the dark spheres are disk clusters. Accreted clusters from different groups are shown by large circles with light gray filling (low-energy group), hexagons with light gray filling (Gaia–Enceladus), gray pentagons (Sagittarius), open asterisks (Sequoia), squares with light gray filling (high-energy group), oblique gray squares (Helmi stream). The green rightward triangles indicate unstratified clusters, the large triangles circumscribe the clusters with an extremely multicomponent Type II stellar population. The gray dots are the current masses of globular clusters (b). The horizontal dashed lines show (a) the average age, (b) average initial mass, and (c, d) traditional dividing line between the disk and the halo at $[\text{Fe}/\text{H}] = -1.0$. The vertical dashed lines: the average radius of the solar orbit (b, d), the line $\text{HBR} = 0.85$ separates extreme blue clusters (c). The clusters mentioned in the text are signed. The $[\text{Fe}/\text{H}]_{\text{H}}$ values are taken from Harris’ catalog [9]. The inclined dashed line is the radial gradient of metallicity (c, d), $[\text{Fe}/\text{H}] = (-0.42 \pm 0.08)R_{\text{sr}} - (0.98 \pm 0.07)$ (d).

of their formation. They were almost unaffected by the destructive influence of the inhomogeneities of our Galaxy’s gravitational potential. As a result, thanks also to their large mass, they were able to retain the gas ejected by their evolved stars and form several stellar populations within them.

The horizontal branch morphological index (HBR)—metallicity diagram for clusters belonging to different groups is depicted in Fig. 1c. The diagram shows that almost all clusters (except ESO452–SC11) with metallicity $-1.5 < [\text{Fe}/\text{H}] < -1.0$ belonging to the bulge and disk lie in a narrow layer above the tilted line drawn “by eye,” which separates the positions of these clusters and accreted ones (see also [5, 6]). Note

that all the clusters of the low-energy group also lie above this line. This fact confirms the assumption that they are genetically related and formed from the same protogalactic cloud, like the bulge and disk clusters. At the same time, as can be seen in Fig. 1c, almost all accreted clusters, including those with an extremely multicomponent stellar population, lie below the tilted line. This behavior of the clusters in the diagram is not surprising, since such a line was first drawn by Zinn [19], separating the clusters lying inside and outside the solar circle. Recall that in [4], the belonging of clusters to the bulge and the disk was limited to a small distance from the galactic center (see above). Thus, the repeatedly stated assumption that metal-poor clusters with anomalously reddened horizontal

branches are of extragalactic origin is confirmed (see [20]).

Figure 1d shows the mean orbital radius–metallicity diagram for all our clusters. This diagram demonstrates the existence of the long-known negative radial metallicity gradient in our Galaxy. It can be seen that the gradient is solely due to the fact that accreted clusters mainly have $[\text{Fe}/\text{H}] < -1.0$ (see the horizontal dashed line), and all genetically related clusters lie within the solar radius (see the vertical dashed line). Five clusters that do not satisfy this condition are noted, and three of them belong to the disrupted Sagittarius galaxy. This galaxy evolved in isolation longer than other disrupted galaxies and reached a higher metallicity. It is clearly seen that among genetically related clusters, half of the bulge clusters and a third of the disk clusters have low metallicities, which are characteristic of accreted clusters. This property of genetically related clusters confirms the conclusion of our study [7] that it is incorrect to distinguish globular clusters as belonging to the subsystem of the thick disk or halo by metallicity $[\text{Fe}/\text{H}] = -1.0$, as it is usually done (see references in [7]). Note that clusters of the low-energy group have the same metallicity range as the in-situ clusters, although the vast majority of them are metal-poor clusters. Nevertheless, this behavior in the diagram is more consistent with genetically related clusters. All clusters with an extremely multicomponent stellar population (except for the former M 54 nucleus) have metallicities close to $[\text{Fe}/\text{H}] \approx -1.5$ and average orbital radii close to the solar galactocentric distance.

4. RELATIONSHIPS BETWEEN ABUNDANCES OF CERTAIN CHEMICAL ELEMENTS AND METALLICITY IN GLOBAL CLUSTERS

4.1. Alpha Elements

Figure 2a shows the $[\text{Fe}/\text{H}]$ – $[\text{Mg}/\text{Fe}]$ diagrams for globular clusters belonging to different groups and field stars of different origin (details below). The lower envelope for genetically related clusters is plotted for the reference as a broken curve drawn “by eye.” In addition to the bulge and disk, the same envelope is also suitable for the low-energy group, which confirms the assumption that its clusters originate from the interstellar gas of the same protogalactic cloud. Both high-energy clusters of known chemistry are also close to this line. On the other hand, a significant part of the clusters of the accreted Gaia–Enceladus, Sequoia, Helmi, and Sagittarius groups are located well below this line. The metal-rich cluster UKS 1, unstratified by the authors of [4], turned out to be among the disk and bulge clusters. It can be seen from Fig. 2a that genetically related clusters and field stars in the low-metallicity range lie in the upper part of the band occupied by all the objects under study.

Figure 2b shows the $[\text{Fe}/\text{H}]$ – $[\text{Si}/\text{Fe}]$ diagram for clusters and field stars. Here, the bulge and disk clusters in the entire metallicity range lie above the field stars (see the lower envelope of these clusters). Recall that the field stars in this diagram are taken from the catalog [13], which includes only genetically related stars of the Galaxy’s disk subsystems. The vast cluster majority of the low-energy group are also above this line. Both clusters from the high-energy group with determined chemical composition here lie close to the lower envelope of genetically related clusters. All clusters of the Sagittarius galaxy in the entire metallicity range turned out to be below the lower envelope. For the rest of the accreted groups, one lower envelope can be drawn even lower. In terms of silicon abundance, the unstratified cluster UKS 1 is also among the genetically related clusters.

Figure 2c depicts the $[\text{Fe}/\text{H}]$ – $[\text{Ca}/\text{Fe}]$ diagram. The calcium abundances in genetically related clusters show a loosely ordered structure, although there are several lines of this element in the visible range and its abundances are determined very reliably. This is mainly expressed in the fact that clusters of all groups occupy the entire width of the band. As a result, the very conditional horizontal lower envelope that we have drawn for genetically related metal-poor clusters turned out to be the same for nearly all clusters. In particular, clusters of low and high energy groups also turned out to be above the drawn line. However, as can be seen from the diagram, some clusters of the Sagittarius group in the entire metallicity range are located much below this line, which means that the lower envelope of this group is lower everywhere. The cluster UKS 1 is at the top of the diagram and has one of the highest calcium abundances $[\text{Ca}/\text{Fe}] = 0.4$.

In Fig. 2d, which shows the $[\text{Fe}/\text{H}]$ – $[\text{Ti}/\text{Fe}]$ diagram, the lower envelope can only be confidently drawn for clusters in the range $[\text{Fe}/\text{H}] > -1.0$. In the less metallic range, the scatter of titanium abundances is so great that the lower envelopes for all groups (except low and high energy groups) should be drawn below all field stars parallel to the abscissa at the value $[\text{Ti}/\text{Fe}] \approx 0.15$. Here, the cluster UKS 1 is also located within the band occupied by genetically related metal-rich clusters.

4.2. Average Abundances of α -Elements

According to modern views, most atoms of all α -elements form in the same processes of nuclear fusion, so it is natural to expect that the relative abundances averaged over magnesium, silicon, calcium, and titanium will turn out to be more reliable than averaged values for any individual element; this will make it possible to correctly represent the differences in the $[\alpha/\text{Fe}]$ ratios in clusters of different groups. The $[\text{Fe}/\text{H}]$ – $[\text{Mg}, \text{Si}, \text{Ca}, \text{Ti}/\text{Fe}]$ diagrams for globular clusters and field stars are shown in Fig. 3a. The num-

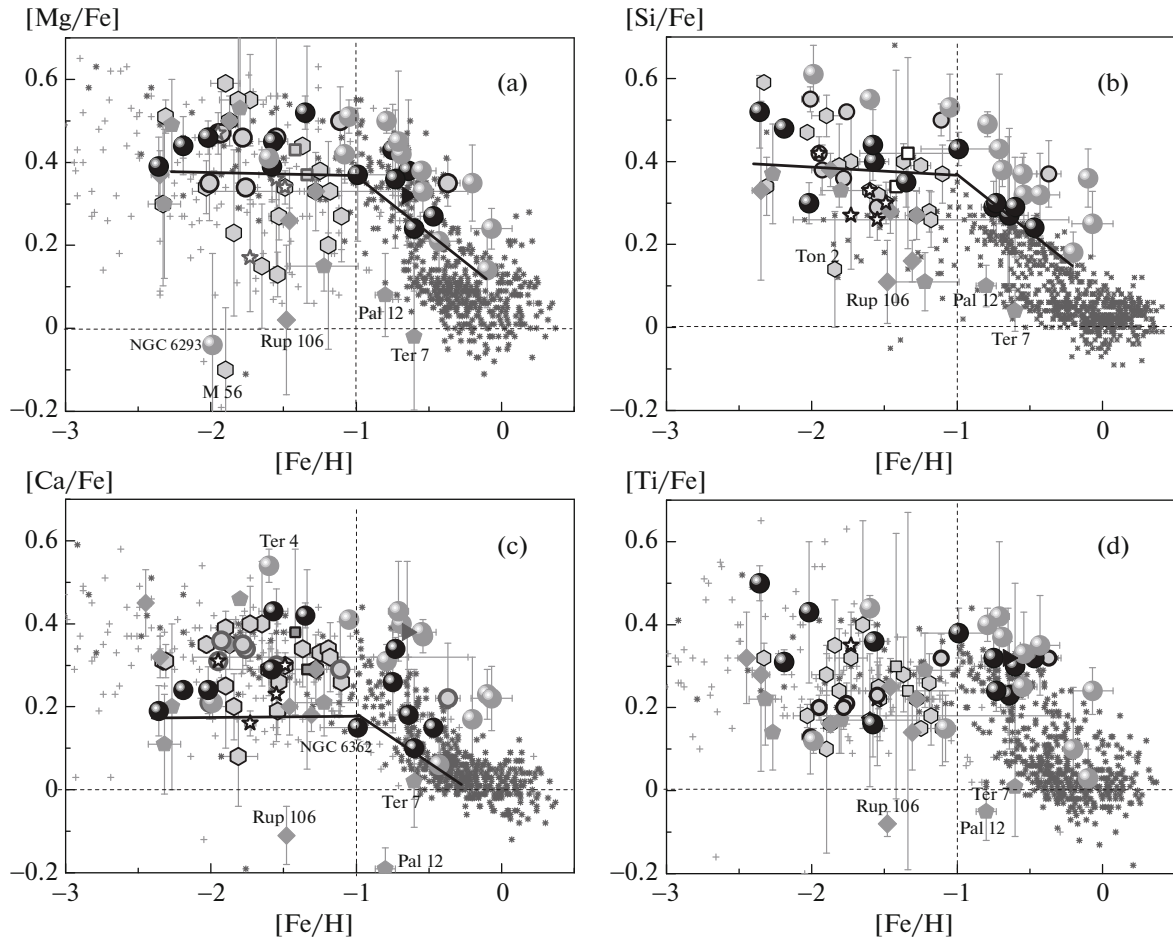


Fig. 2. Dependence of the relative abundances of magnesium (a), silicon (b), calcium (c), and titanium (d) versus metallicity for the globular clusters of our catalog and field stars from the catalogs [12] (a, c, d) and [13] (b). The notations of the globular clusters and field stars are the same as in Fig. 1. The dark snowflakes are genetically related field stars with $V_{\text{res}} < 240$ km/s; the light gray crosses are high-velocity field stars (b). The horizontal dashed lines are drawn through the solar relative abundances of the elements, and the vertical lines through the dividing value $[\text{Fe}/\text{H}] - 1.0$. The bars indicate the authors' averaged errors in determining the abundances for the globular clusters. The broken curves are the lower envelopes drawn “by eye” for genetically related clusters.

ber of clusters here is slightly less than for individual elements, but the reliability of the average values is higher. In the figure, this is manifested in the fact that the bands occupied by both field stars and globular clusters are noticeably narrower, and the differences in the cluster positions of different groups and stars of different origin are more distinct.

For genetically related field stars and clusters, i.e., those formed from the same protogalactic cloud, metallicity can serve as a statistical indicator of their age, since the total abundance of heavy elements in a closed star–gas system (which our Galaxy can be considered in the first approximation) is steadily increasing over time. We assume that such are the field stars with a residual velocity $V_{\text{res}} < 240$ km/s (see [21]) (they are indicated in the diagram by small dark snowflakes). The vast majority of field stars with higher residual velocities (marked with gray crosses) have ret-

rograde rotation (see [21, Fig. 3a]). All higher-velocity stars can be considered accreted candidates. Note that metal-poor ($[\text{Fe}/\text{H}] < -1.0$) genetically related field stars are located along the upper half of the band in our $[\text{Fe}/\text{H}] - [\alpha/\text{Fe}]$ diagrams, and this confirms the conclusion of [22] that metal-poor field stars with low relative abundances of α -elements are accreted. Those authors drew the dividing line at $[\alpha/\text{Fe}] \sim 0.3$ for stars with $[\text{Fe}/\text{H}] < -1.0$. We have also drawn the lower envelope “by eye” (as a gray broken line) as a reference for genetically related stars; the position of this line, as we can see, nearly coincides with the one proposed by the authors of [22]. As for the position of metal-rich ($[\text{Fe}/\text{H}] > -1.0$) globular clusters in the $[\text{Fe}/\text{H}] - [\alpha/\text{Fe}]$ diagrams, we described it in detail in [7].

The dark broken “by eye” line in the figure shows the lower envelope for the clusters called in situ in [4].

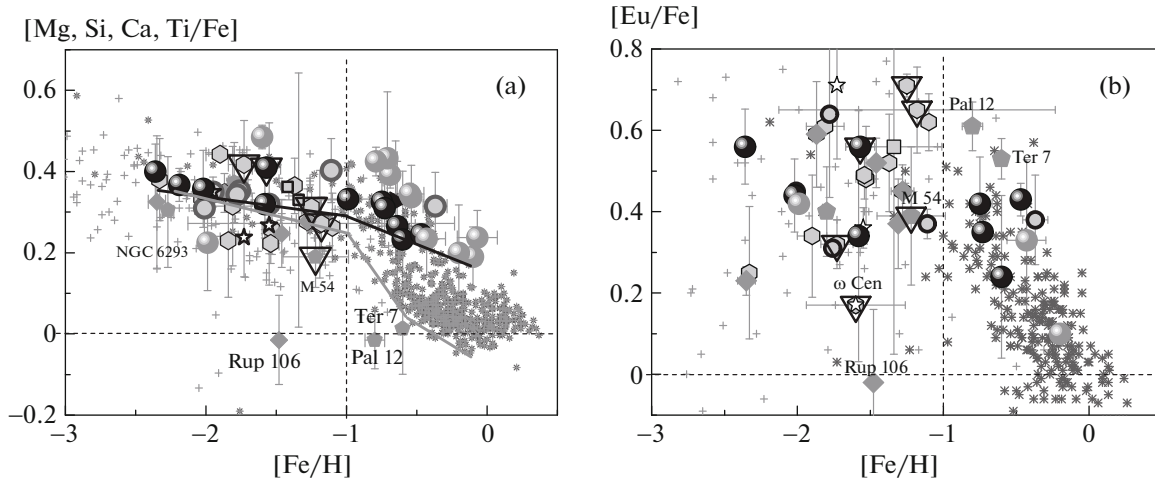


Fig. 3. Dependence of the relative abundances averaged over four α -elements (Mg, Si, Ca, Ti) (a), and the rapid neutron capture element (Eu) (b) versus metallicity for globular clusters and field stars from the catalog [12] (due to the absence of silicon abundances for field stars, the $[\alpha/\text{Fe}]$ ratios in panel (a) are obtained for three elements). The notations are the same as in Figs. 1 and 2. The broken lines are the lower envelopes drawn “by eye” for genetically related globular clusters (black) and field stars (gray).

Approximately in the same place, there is also the lower envelope in the low-metallicity range drawn “by eye” as a gray line for genetically related field stars. Only the bulge cluster NGC 6293 turned out to be in the low-metallicity range much below this line. The silicon abundances in this cluster were the highest among the clusters, while all other elements invariably show low relative abundances. We can see that almost all clusters from the low-energy group and also, possibly, from the high-energy group (however, there are only two of the latter with chemical composition) also lie above the drawn line. It turns out that clusters with certain relative abundances of α -elements from the low-energy group, as well as from the high-energy group, confidently stay among genetically related clusters. Most clusters of all other accreted groups lie below this line. The average abundance of four alpha elements in metal-poor genetically related clusters $\langle [\alpha/\text{Fe}] \rangle = 0.36 \pm 0.03$, while for accreted clusters it is less outside the error limits and amounts to 0.29 ± 0.02 . These values coincide with those for the field stars: 0.34 ± 0.02 and 0.29 ± 0.01 , respectively.

Despite the small number, it can be seen that the clusters of the Sagittarius (Sgr) group form a rather narrow band, which in the entire metallicity range lies below the lower envelope for genetically related field stars (see the gray broken line) and below the lower envelope for genetically related globular clusters. The only cluster UKS 1 with known relative abundances of α -elements, that could not be stratified by the authors of [4], fell into the metal-rich cluster region of the disk and bulge. It is also seen that globular clusters with an extremely multicomponent population at rather close metallicities show a significant difference in the relative abundances of α -elements.

4.3. Rapid Neutron Capture Elements

Figure 3b shows the diagrams of the relative abundances of a rapid neutron capture element (europium) versus metallicity for globular clusters belonging to different groups, as well as field stars. It is known that rapid neutron capture elements form in the outbursts of the least massive Type II supernovae with masses $(8-10) M_{\odot}$, and some of these atoms form as a result of the merger of neutron stars [23]. Since α -elements are also ejected into the interstellar medium by SNe II (albeit with masses $>10 M_{\odot}$), the $[\text{Fe}/\text{H}] - [\alpha/\text{Fe}]$ and $[\text{Fe}/\text{H}] - [\text{Eu}/\text{Fe}]$ diagrams are quite similar integrally. However, the $[\text{Eu}/\text{Fe}]$ ratios in the low-metallicity range for clusters with different origin do not show a clear difference in positions similar to those noted for $[\alpha/\text{Fe}]$. Here, the clusters of all groups are mixed, and only two accreted clusters fall down far outside the error limits, ω Cen and Rup 106. However, it can be noted that the highest $[\text{Eu}/\text{Fe}]$ ratios in this range are demonstrated not by genetically related, but by accreted clusters (mainly from the Gaia–Enceladus galaxy). At the same time, in the range of $[\text{Fe}/\text{H}] > -1.0$, clusters of the bulge, disk, and low-energy group form a sequence at the top of the field star band.

Note that both metal-rich clusters from the Sagittarius galaxy, Pal 12 and Ter 7, turned out to have the highest $[\text{Eu}/\text{Fe}]$ ratios. Possibly, the position of the $[\text{Eu}/\text{Fe}]$ ratios that are opposite to relative abundances of α -elements is due to the fact that interstellar matter in the Sagittarius dwarf galaxy was most likely enriched mainly by low-mass SNe II supernovae, which are the main suppliers of rapid neutron capture elements. As a result, we can see that these clusters in this galaxy have a deficit of α -elements and excess of

r -elements. However, this assumption requires additional research.

5. DISCUSSION

Let us list the main properties of globular clusters that formed, according to the authors of [4], in situ, i.e., the bulge and disk clusters. All of them are in orbits, the average radii of which are smaller than the solar orbital radius (see Figs. 1b, 1d). In addition to being older than accreted clusters given the same metallicity (see Fig. 1a), these clusters on average turn out to have higher relative abundances of α -elements (see Figs. 2, 3a). As a rule, disk and bulge clusters have predominantly large initial masses (see Fig. 1b), since all less massive clusters near the galactic center have already completely dissipated into separate stars. In addition, metal-rich clusters of these groups have extremely red horizontal branches, while for clusters with low metallicity they are extremely blue (Fig. 1c). The bulge clusters (and one disk cluster) with intermediate metallicity ($-1.3 < [\text{Fe}/\text{H}] < -0.9$) have horizontal branches of intermediate color. It turns out that the combination of all the listed properties is inherent for clusters that formed within the same protogalactic cloud, i.e., are genetically related.

It turned out that the low-energy clusters that were classified by the authors of [4] as accreted, also have nearly all the properties listed above. Therefore, we conclude that they are actually genetically related, despite the fact that all of them lie in the band occupied by accreted clusters in the metallicity–age diagram, and some of them turned out to be younger than genetically related clusters with the same metallicity (see Fig. 1a). The authors of [24] came to the same conclusion based on the discovery of high relative silicon abundances in these clusters from the SDSS-APOGEE data. It can be assumed that the clusters of this group formed slightly later than the others from isolated protogalactic fragments. Of course, this assumption needs to be verified by numerical modeling. The metal-rich cluster UKS 1, non-stratified in [4], in which the abundances of all α -elements are the same as those of the bulge and disk clusters, most likely also belongs to the genetically related. As can be seen from Fig. 1b, since its mass is more than a million solar masses, and, from Fig. 1d, the average radius of its orbit ≈ 0.7 kpc, it belongs to the bulge. In addition, the small average radius of the orbit and the large mass of the Liller 1 cluster, not stratified in [4], suggests that it, too, most likely belongs to the bulge (see also [24]); however, the very distant low-mass cluster (AM 4) is almost certainly of extragalactic origin.

The clusters of all other groups show, on average, noticeably lower relative abundances of α -elements (see Figs. 2 and 3a), which implies that they were born in galaxies of lower masses than our Galaxy. Moreover, it is unlikely that the low values of the $[\alpha/\text{Fe}]$

ratios in accreted clusters can be explained only by the lower rate of star formation in these disrupted dwarf galaxies (as is usually believed), since a significant number of young accreted clusters, as well as genetically related ones, have high relative abundances of α -elements. In addition, the relative abundances of europium show no such trend. Most likely, the spread is simply due to the poor mixing of the interstellar medium in dwarf galaxies, where SNe II of different masses flare up in different places. It seems more reasonable to explain the observed overestimation on average by higher masses of type II supernovae in our very massive Galaxy. Indeed, on the one hand, according to modern views, the yield of α -elements increases with increasing mass of the presupernova (see, e.g., [25]). On the other hand, it is known that low-mass supernova explosions are more likely to occur in low-mass dwarf galaxies [26]. However, the masses of the dwarf galaxies that supplied globular clusters to our Galaxy were in fact much larger than the masses of the dwarf satellite galaxies surrounding it at the present time (see, in particular, [5, 6, 27]). This conclusion was made on the basis that the values of the $[\alpha/\text{Fe}]$ ratios in the stars of the surviving dwarf satellite galaxies are substantially less than in globular clusters and field stars that currently belong to our Galaxy (see, e.g., [6]). Indeed, as shown by satellite measurements of the distances and velocities of stellar objects, the masses of galaxies accreted 10 Gyr ago were rather large, but less than that of our Galaxy. We have already noted above that the mass of the dwarf galaxy Gaia–Enceladus, according to the authors of [3], significantly exceeds the mass of the Small Magellanic Cloud, just the stellar mass in which reaches $\approx 5 \times 10^9 M_{\odot}$. The stellar mass in the Sequoia galaxy is $\sim 5 \times 10^7 M_{\odot}$, while the total mass is $\sim 10^{10} M_{\odot}$ [2]. Modeling the tidal tail kinematics of the stars of the Sagittarius galaxy in [28] showed that, in order to reproduce the velocity dispersion in the stream from this galaxy, the mass of its dark halo should be $M = 6 \times 10^{10} M_{\odot}$. The masses of other disintegrated galaxies that formed the groups of clusters studied here (Sequoia, High Energy, and Helmi streams 99) are only slightly less than the masses of those listed (see [29] and references therein). As a result, it turns out that our Galaxy accreted the most massive satellite galaxies at the early stages of its formation, while the least massive ones still continue to exist autonomously.

At the same time, the disrupted dwarf galaxies, along with the already known decrease in the lower limit of the initial masses of the clusters with distance from the galactic center, revealed another interesting property: they have almost no globular clusters of large masses (see Fig. 1d). Only a few clusters are exceptions, and two of them are the central clusters of these former galaxies. Moreover, the upper mass limit

decreases with an increase in the average orbital radii of the clusters. This decrease can no longer be explained by the destruction of clusters. Numerical modeling shows that rather massive satellite galaxies begin to be intensively disrupted by the tidal forces of the Galaxy only after a significant decrease in the size of their orbits, while less massive ones are disrupted even at distant approaches to our Galaxy [30]. In this case, the least massive clusters are lost by dwarf galaxies in the first place, so they mostly remain in distant orbits. Based on the foregoing, we can assume that the lower the mass of the host galaxy, the lower the maximum masses of the globular clusters formed in it.

Finally, a number of the most massive clusters of disrupted dwarf galaxies exhibit extremely multicomponent Type II stellar populations (see Fig. 1). Among them are: the central clusters of Sequoia (ω Cen) and Sagittarius (M 54) galaxies; 4 clusters from the most massive disrupted galaxy Gaia–Enceladus; and the most metal-poor cluster of this group, the disk cluster M 22, whose horizontal branch only slightly differs from the extreme blue. Moreover, all these clusters are less than 12.5 Ga in age and have intermediate metallicity ($-1.7 < [\text{Fe}/\text{H}] < -1.2$) and average radii, approximately equal to the solar orbital radius. The formation of extremely multicomponent stellar populations in massive accreted clusters can be explained by the fact that they evolved for a long time far from the destructive influence of the inhomogeneities of the our Galaxy’s gravitational potential and, as a result, preserved all the enriched matter released by their evolved stars, from which new generations of stars formed.

ACKNOWLEDGMENTS

The authors are grateful to Davide Massari for providing the unpublished ages of the globular clusters and Holger Baumgardt for providing the updated initial globular cluster masses.

FUNDING

The research was funded by the Southern Federal University, 2020 (Ministry of Science and Higher Education of the Russian Federation).

REFERENCES

1. R. Ibata, G. Gilmore, and M. Irwin, *Nature* (London, U.K.) **370**, 194 (1994).
2. J. T. Mackereth, R. P. Schiavon, J. Pfeffer, C. R. Hayes, et al., *Mon. Not. R. Astron. Soc.* **482**, 3426 (2019).
3. A. Helmi, C. Babusiaux, H. H. Koppelman, D. Massari, J. Veljanoski, and A. G. A. Brown, *Nature* (London, U.K.) **563**, 85 (2018).
4. D. Massari, H. H. Koppelman, and A. Helmi, *Astron. Astrophys.* **630**, 4 (2019).
5. V. A. Marsakov, V. V. Koval’, and M. L. Gozha, *Astron. Rep.* **63**, 274 (2019).
6. V. A. Marsakov, V. V. Koval’, and M. L. Gozha, *Astrophys. Bull.* **74**, 404 (2019).
7. V. A. Marsakov, V. V. Koval’, and M. L. Gozha, *Astrophys. Bull.* **75**, 21 (2020).
8. T. Bensby, S. Feltzing, and I. Lundstrom, *Astron. Astrophys.* **410**, 527 (2003).
9. W. E. Harris, *Astron. J.* **112**, 1487 (1996); arXiv:1012.3224 [astro-ph.GA].
10. E. Carretta, in *The General Assembly of Galaxy Halos: Structure, Origin and Evolution*, Ed. by A. Bragaglia, M. Arnaboldi, M. Rejkuba, and D. Romano, *Proc. IAU Symp.* **317**, 97 (2016).
11. J. Pritzl, K. A. Venn, and M. Irwin, *Astron. J.* **130**, 2140 (2005).
12. K. A. Venn, M. Irwin, M. D. Shetrone, C. A. Tout, V. Hill, and E. Tolstoy, *Astron. J.* **128**, 1177 (2004).
13. T. Bensby, S. Feltzing, and M. S. Oey, *Astron. Astrophys.* **562**, 71 (2014).
14. D. A. Vandenberg, K. Brogaard, R. Leaman, and L. Casagrande, *Astrophys. J.* **775**, 134 (2013).
15. E. Carretta, A. Bragaglia, R. Gratton, V. d’Orazi, and S. Lucatello, *Astron. Astrophys.* **508**, 695 (2009).
16. A. F. Marino, A. P. Milone, A. Renzini, F. D’Antona, et al., *Mon. Not. R. Astron. Soc.* **487**, 3815 (2019).
17. H. Baumgardt, M. Hilker, A. Sollima, and A. Bellini, *Mon. Not. R. Astron. Soc.* **482**, 5138 (2019).
18. T. V. Borkova and V. A. Marsakov, *Bull. SAO* **54**, 61 (2002).
19. R. Zinn, in *The Globular Cluster-Galaxy Connection*, Ed. by H. Smith and J. Brodee, *ASP Conf. Ser.* **48**, 38 (1993).
20. G. S. da Costa and T. E. Armandroff, *Astron. J.* **109**, 253 (1995).
21. V. A. Marsakov and T. V. Borkova, *Astron. Lett.* **32**, 545 (2006).
22. P. E. Nissen and W. J. Schuster, *Astron. Astrophys.* **511**, L10 (2010).
23. J. J. Cowan, C. Sneden, J. E. Lawler, A. Aprahamian, M. Wiescher, K. Langanke, G. Martinez-Pinedo, and F.-K. Thielemann, arXiv:1901.01410 [astro-ph.HE] (2010).
24. D. Horta, R. P. Schiavon, J. T. Mackereth, T. C. Beers, et al., *Mon. Not. R. Astron. Soc.* **493**, 3363 (2020).
25. C. Travaglio, D. Galli, R. Gallino, M. Busso, F. Ferrini, and O. Straniero, *Astrophys. J.* **521**, 691 (1999).
26. J. Köppen, C. Weidner, and P. Kroupa, *Mon. Not. R. Astron. Soc.* **375**, 673 (2007).
27. J. Pritzl, K. A. Venn, and M. Irwin, *Astron. J.* **130**, 2140 (2005).
28. S. L. J. Gibbons, V. Belokurov, and N. W. Evans, *Mon. Not. R. Astron. Soc.* **464**, 794 (2017).
29. H. H. Koppelman, A. Helmi, D. Massari, A. M. Price-Whelan, and T. K. Starkeburg, *Astron. Astrophys.* **631**, L9 (2019).
30. M. G. Abadi, J. F. Navarro, M. Steinmetz, and V. R. Eke, *Astrophys. J.* **591**, 499 (2003).

Translated by M. Chubarova